Supplementary Information

"Mice alternate between discrete strategies during perceptual decision-making"

Ashwood *et al*, 2021

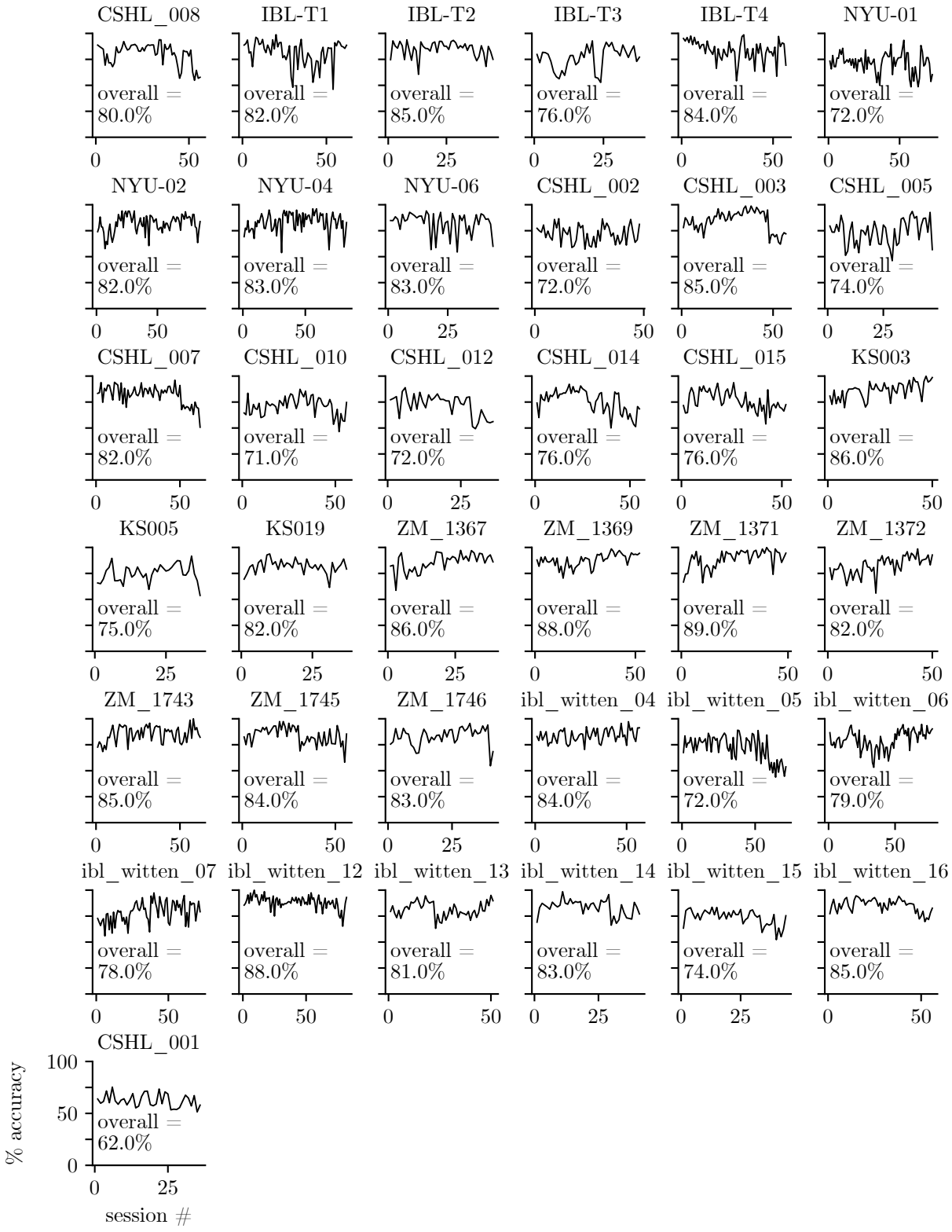

Figure S1: **Raw behavioral data for IBL animals: Accuracy across sessions.** We plot the accuracy of IBL animals [1] across sessions as evidence that mice have learned the task, and that their choice behavior has reached stationarity. We also report the overall accuracy of each animal when aggregated across sessions. The example animal studied in Fig. 2 and Fig. 3 is 'CSHL_008'.

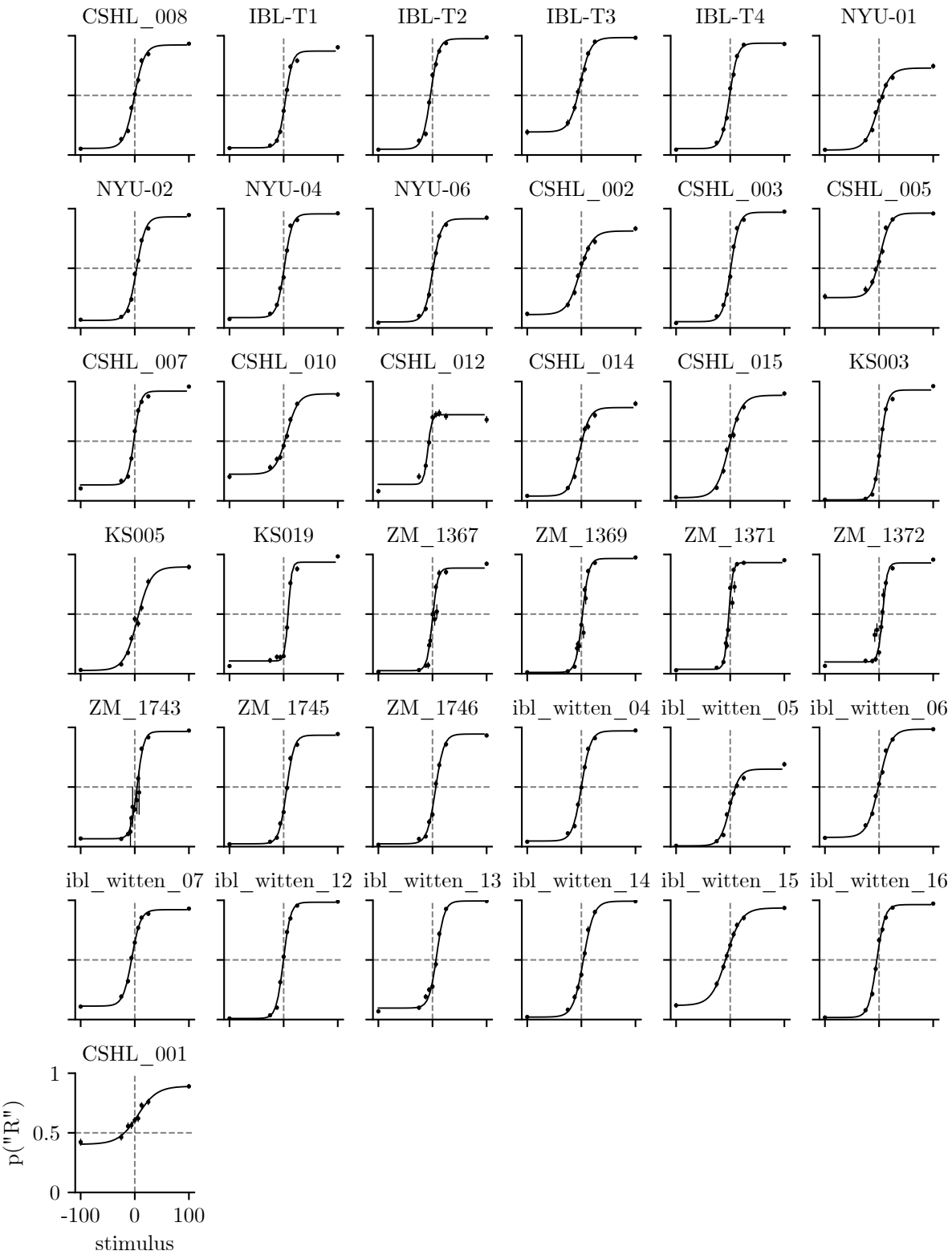

Figure S2: **Raw behavioral data for IBL animals: Psychometric curves.** We plot the psychometric curves for the 37 IBL animals [1] whose choice data we study. The example animal that we study in Fig. 2 and Fig. 3 is 'CSHL_008'. Animals are ordered in the same way that they are in Fig. S1 when considering row-major order, so plots can be compared across the two figures. In each plot, we also show each animal's empirical choice probabilities; error bars are 68% confidence intervals (minimum n for animal-stimulus pair was 6, while maximum was 1547. Median n was 493).

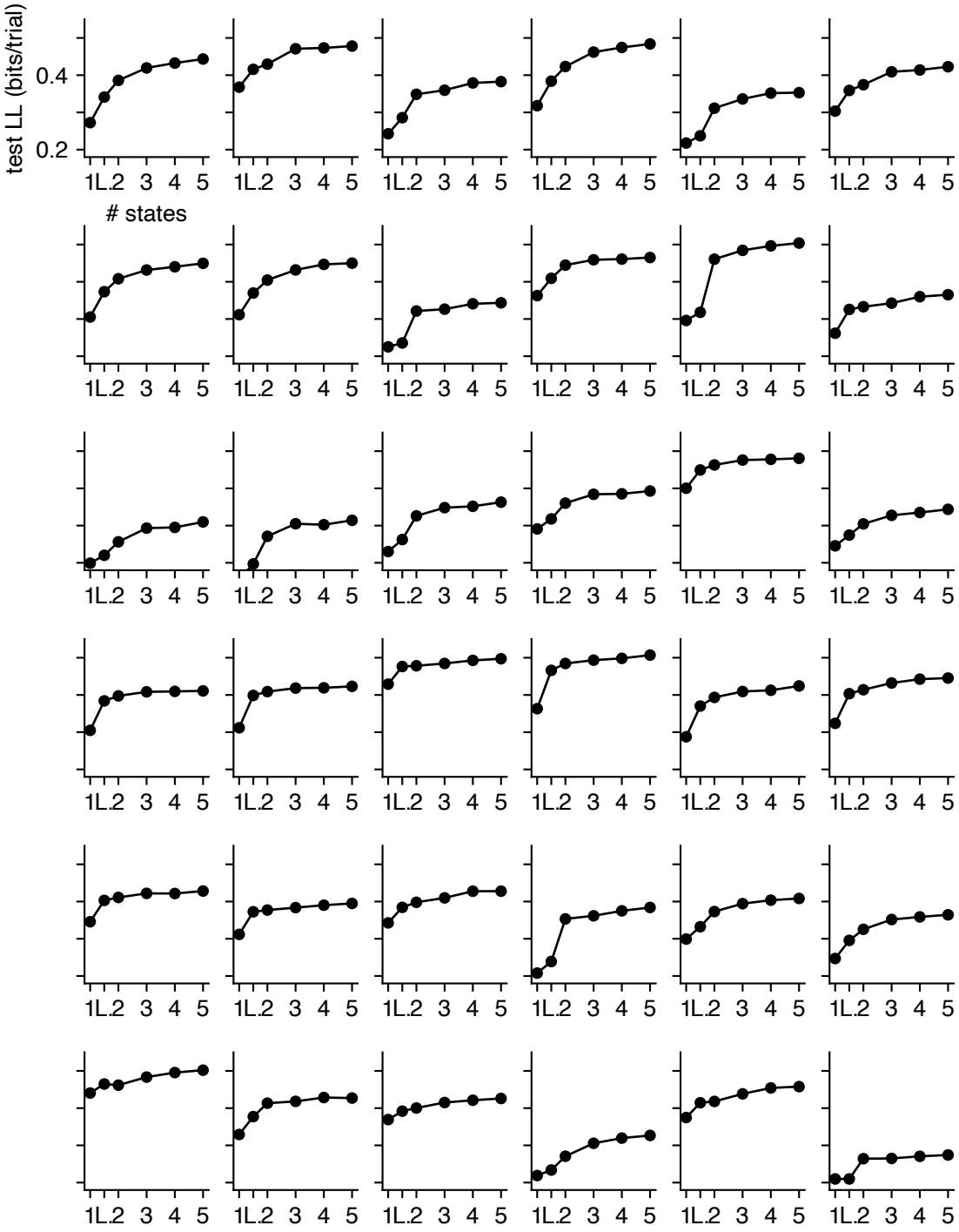

Figure S3: **Model comparison for all IBL animals** Rather than plotting curves on top of one another as in Fig. 4a, we plot each individual animal's test set loglikelihood in a grid. We do not show model comparison results for the example animal studied in Fig. 2 and Fig. 3 since we show the curve for that particular animal there, but animals are otherwise ordered in the same way (according to row-major order) that they are in Fig. S1 and Fig. S2, so plots can be compared across these figures.

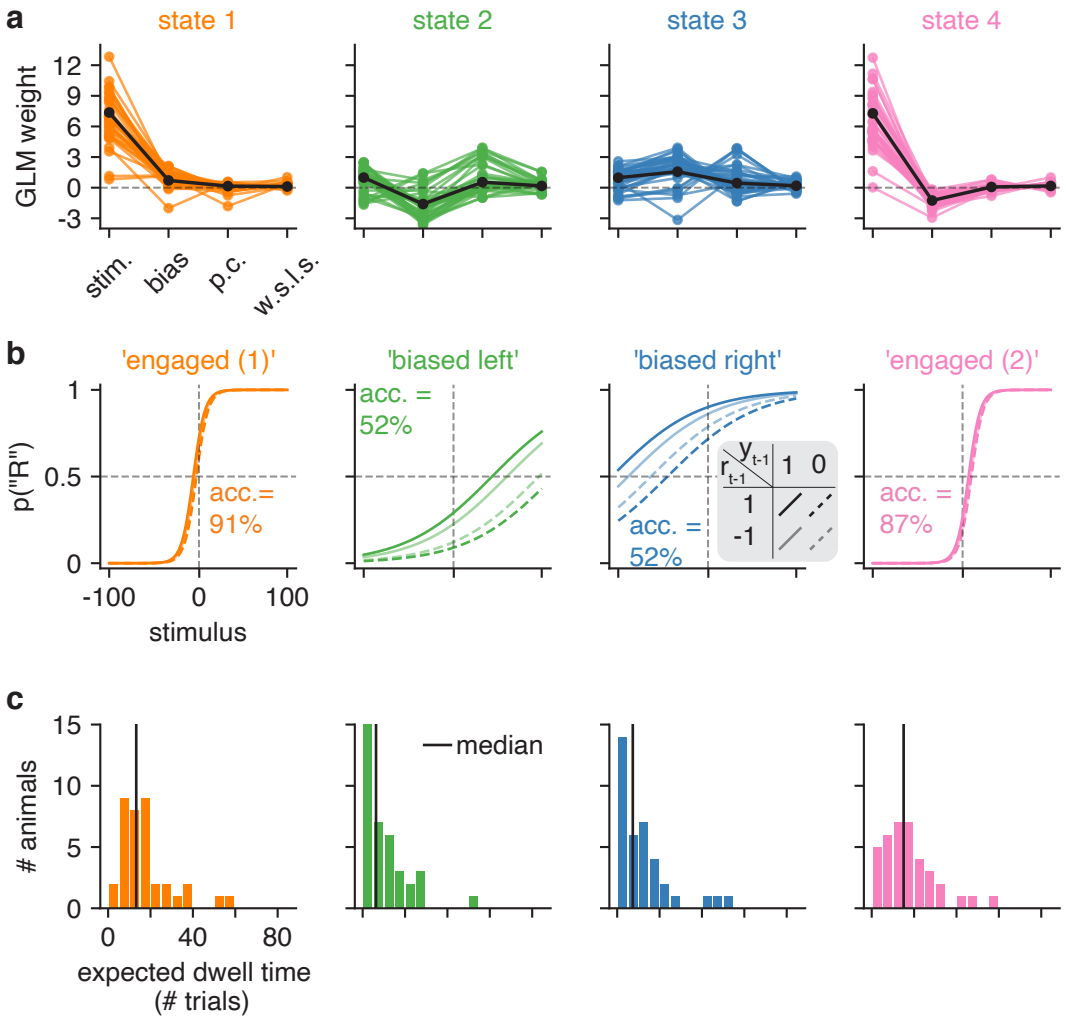

Figure S4: **GLM-HMM 4 state fits to IBL data.** **(a)** Retrieved GLM weights for each of the 37 IBL animals for each state of the 4 state GLM-HMM, as well as the global weights (black) for the fit when all data from all animals are concatenated. **(b)** An alternative method of plotting the weights in panel a: we plot, as a function of the stimulus intensity, as well as the animal's reward and choice on the previous trial, the probability that the animal goes rightward at the current trial. **(c)** The expected dwell time for each animal in each of the 4 states, as obtained from the best-fitting transition matrices for each animal.

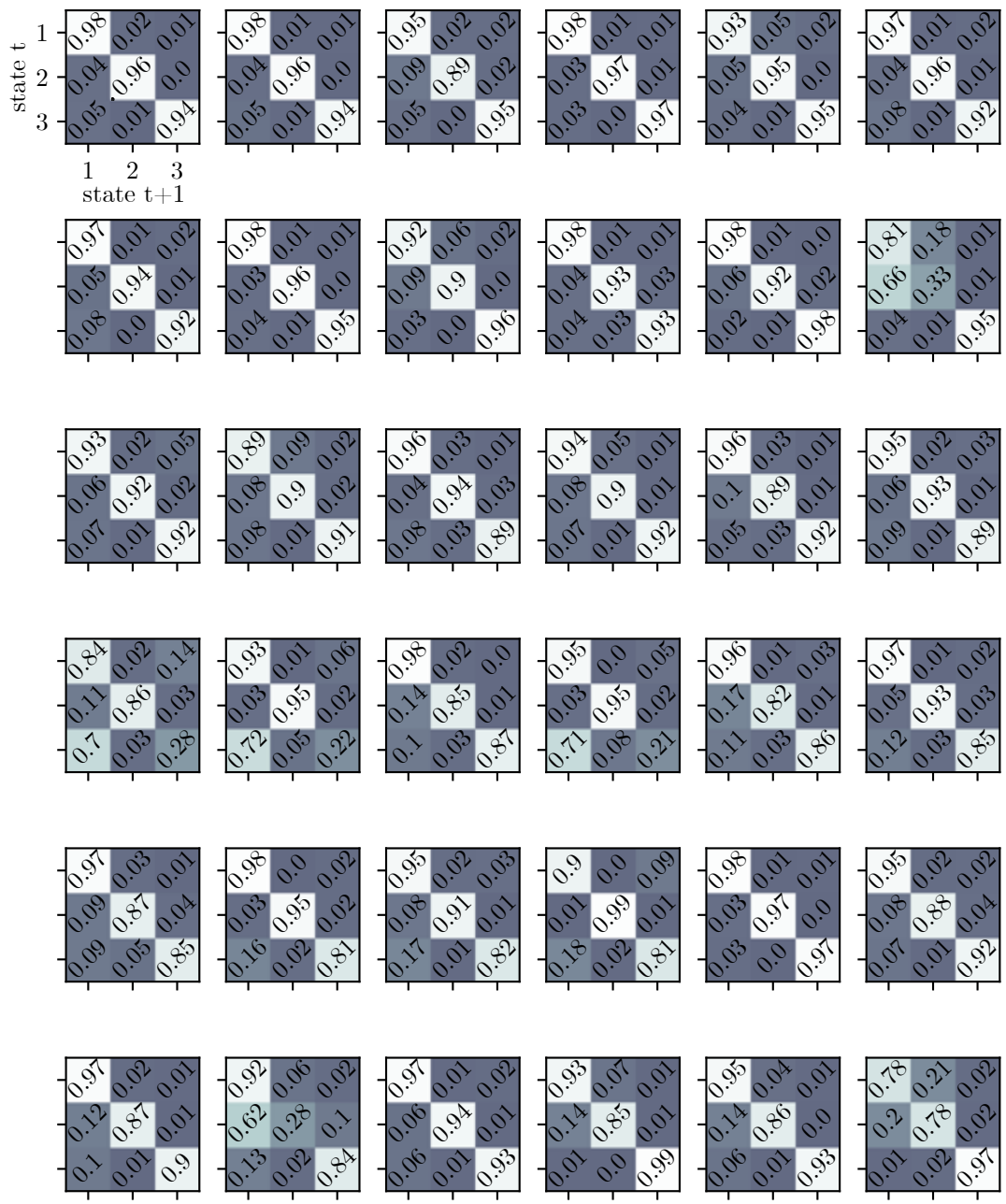

Figure S5: **Retrieved transition matrices for all IBL animals** We do not plot the transition matrix for the example animal studied in Fig. 2 as the retrieved transition matrix is shown there. Animals are ordered in the same way as in other supplemental figures so plots can be compared across figures.

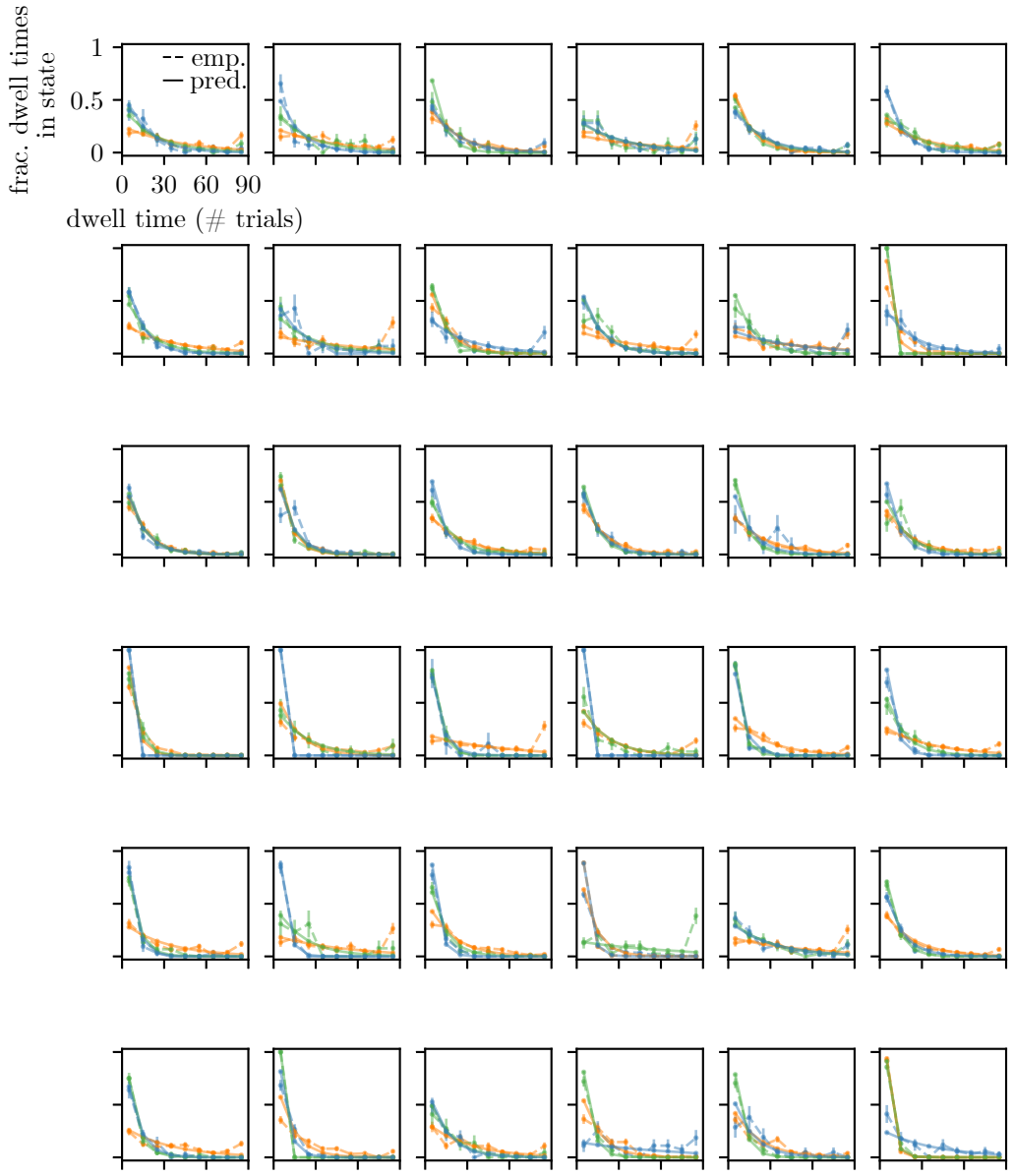

Figure S6: **State dwell times are approximately geometrically distributed for all IBL animals.** We plot the predicted ("pred."; shown with the solid line) and empirical ("emp."; shown with the dashed lines) state dwell time probabilities for each IBL animal and each state (excluding the example animal since the state dwell time probabilities for the example animal are shown in Fig. ED2)). Colors map to states in the usual way (orange is state 1, green is state 2, blue is state 3). The empirical state dwell times are obtained by using the posterior state probabilities to assign state labels to trials. 68% confidence intervals are shown for empirical values (median n for an animal-state pair was 75; minimum n was 9; maximum n was 419). Predicted state dwell time probabilities are obtained from the transition matrix according to $p(\text{dwell time} = t) = (1 - A_{kk})A_{kk}^{t-1}$.

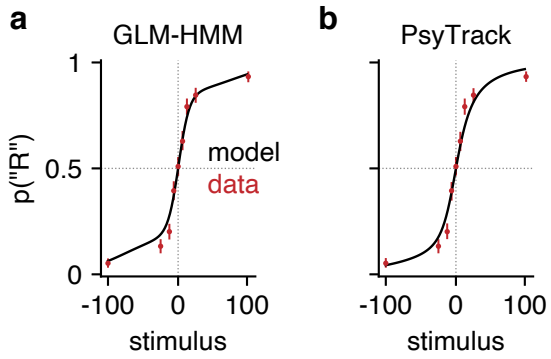

Figure S7: **GLM-HMM and PsyTrack model fits to choice data from example mouse. (a)** Copy of Fig. 2h illustrating the psychometric curve generated by the GLM-HMM for the example mouse studied in Fig. 2 and Fig. 3. Specifically, using the fit GLM-HMM parameters for this animal and the true sequence of stimuli presented to the mouse, we generated a time series with the same number of trials as those that the example mouse had in its dataset. At each trial, regardless of the true stimulus presented, we calculated $p_t(\text{“}R\text{”})$ for each of the 9 possible stimuli by averaging the per-state psychometric curves of Fig. 2g and weighting by the appropriate row in the transition matrix (depending on the sampled latent state at the previous trial). Finally, we averaged the per-trial psychometric curves across all trials to obtain the curve that is shown in black, while the empirical choice data of the mouse are shown in red, as are 95% confidence intervals (n between 530 and 601 depending on stimulus). **(b)** Ability of PsyTrack model to fit the empirical choice data (red dots with 95% confidence intervals (n between 530 and 601 depending on stimulus)) for the same example mouse. We again obtained a per-trial psychometric curve using the per-trial weights returned by the PsyTrack model of [2, 3] and used these to evaluate $p_t(\text{“}R\text{”})$ for each of the 9 possible stimuli. Again, the black line represents the average curve across all trials. Note: despite the absence of explicit lapse parameters in this model, it is able to capture the non-zero error rate of the mouse on “easy” trials.

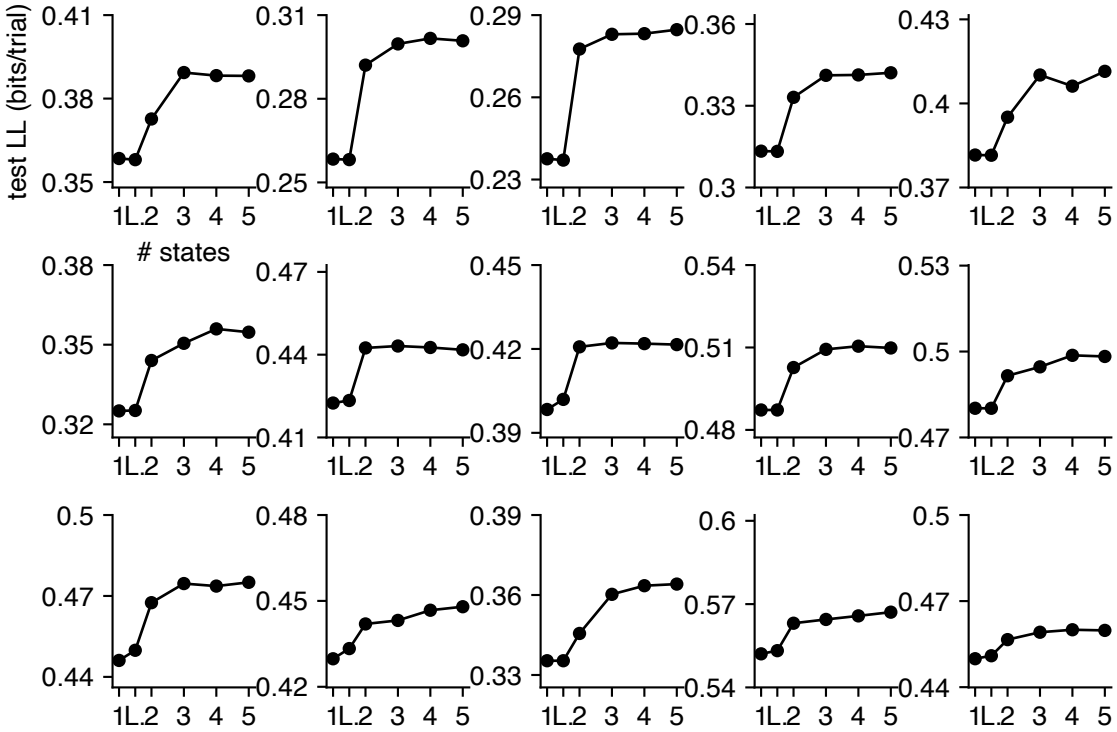

Figure S8: **Model Comparison for all Odoemene et al. animals.** Rather than plotting curves on top of one another as in Fig. 5b, we plot each individual animal's test set loglikelihood in a grid. Animals are ordered in the same way that they are in Fig. S13 and Fig. S14, so plots can be compared across figures.

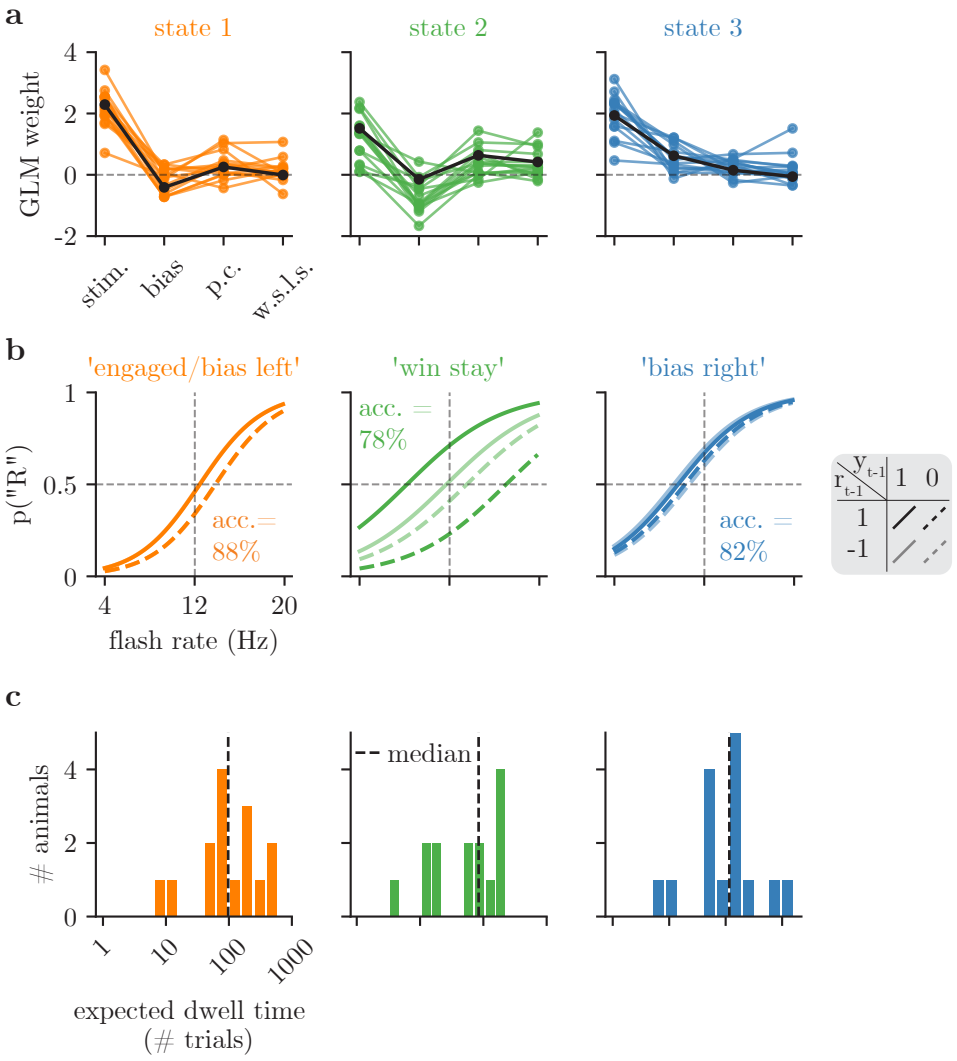

Figure S9: **GLM-HMM 3 state fits to Odoemene et al. data.** When 3 state GLM-HMMs are fit to the Odoemene et al. data, the engaged and bias left states are merged to form a single (mostly engaged) state (accuracy remains high at 88%), while the win-stay and bias right states are largely unchanged. This is a sister figure to panels d, e, and f of Fig. 5, where the panels can be interpreted in the same way that they are there.

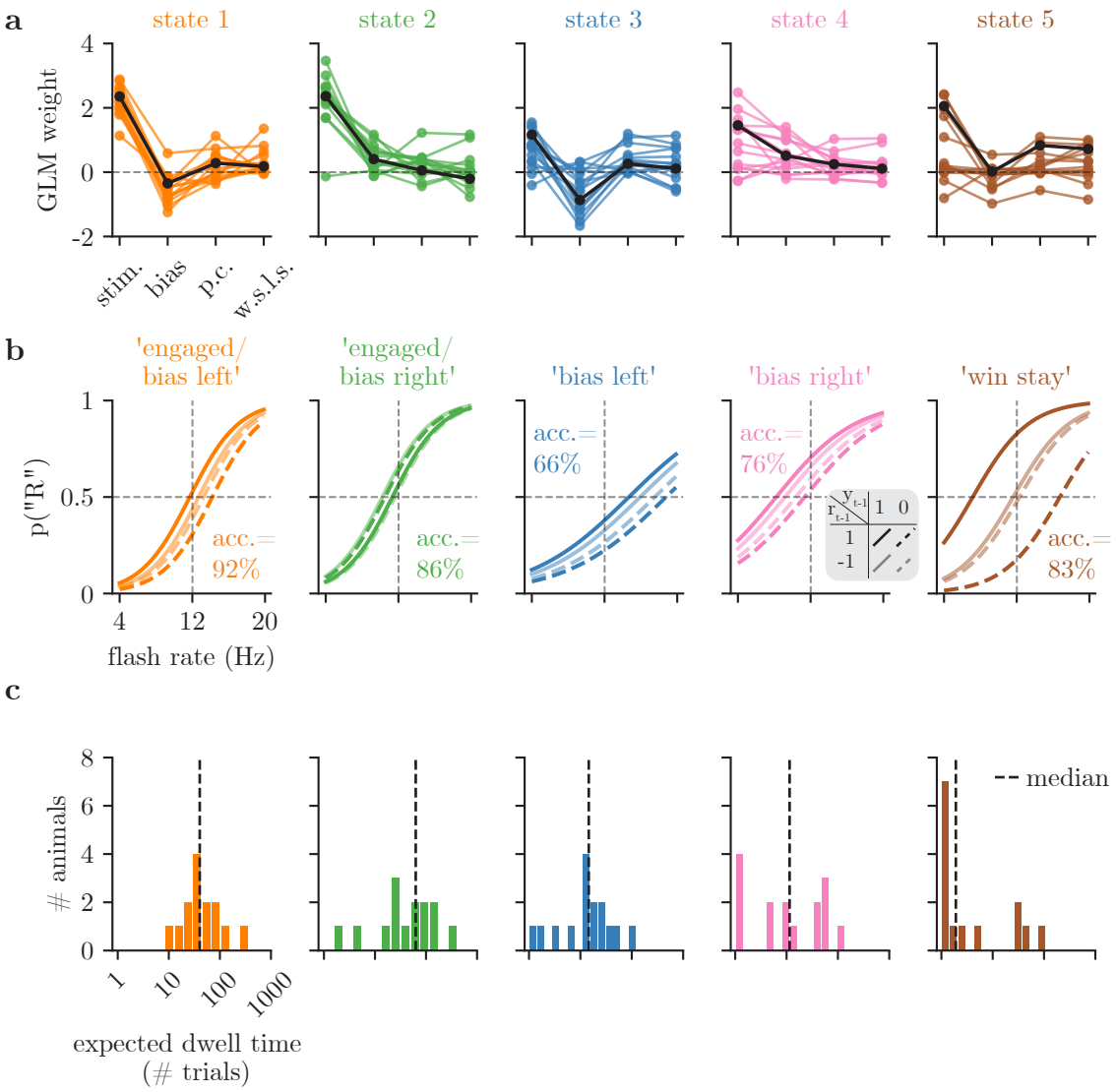

Figure S10: **GLM-HMM 5 state fits to Odoemene et al. data.** When 5 state GLM-HMMs are fit to the Odoemene et al. data, the engaged state is split into an engaged/bias left and engaged/bias right state, while the win-stay, bias right and bias left states are largely unchanged. This is a sister figure to panels d, e, and f of Fig. 5, where the panels can be interpreted in the same way that they are there.

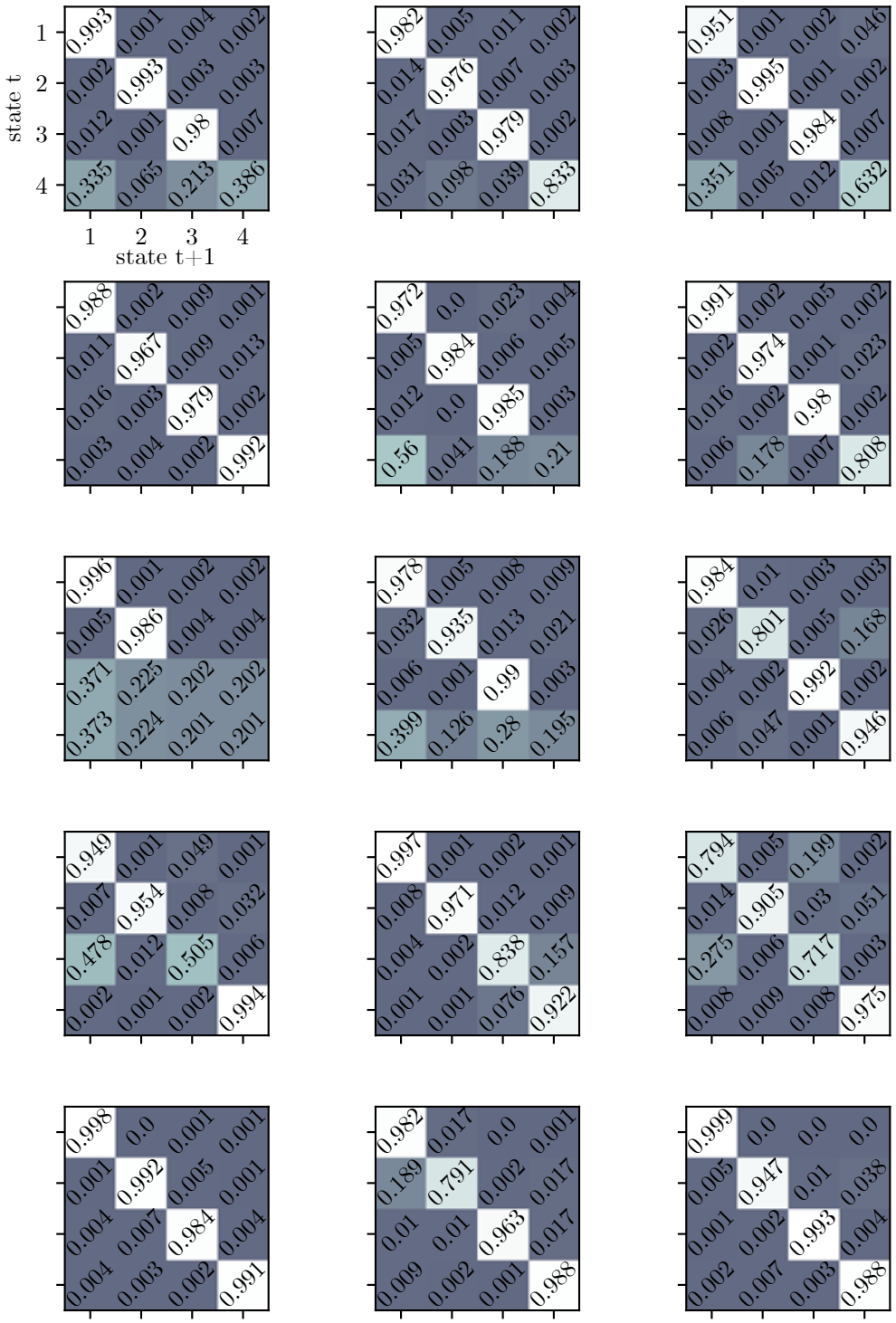

Figure S11: **Retrieved transition matrices for Odoemene et al. animals** Each individual transition matrix is the best fitting transition matrix for 1 of the 15 Odoemene et al. mice that we study. Row-major order has animals ordered in the same way that they are in Fig. S8.

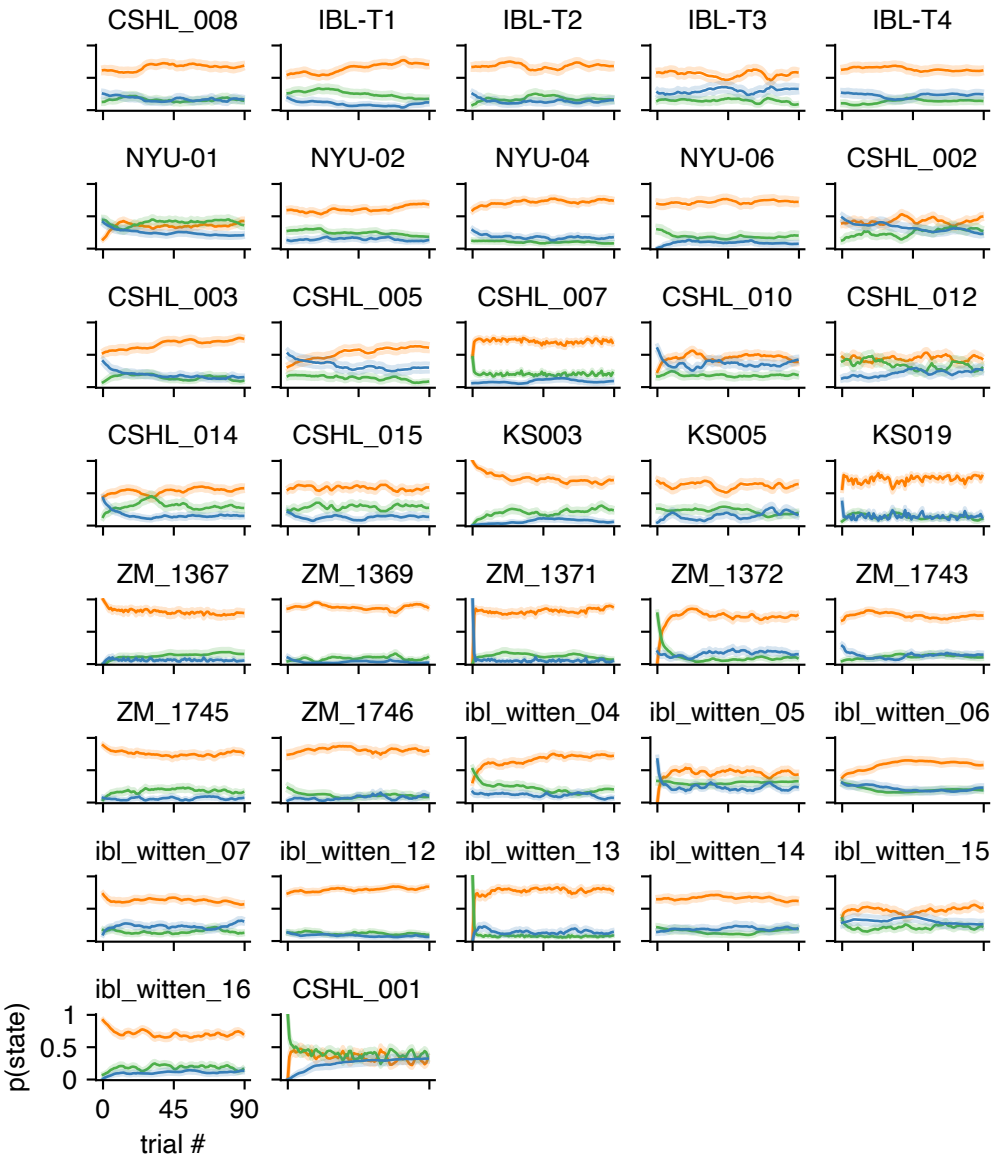

Figure S12: **Average posterior state probabilities for all IBL animals.** Average posterior state probabilities across all sessions for each individual animal along with 68% confidence intervals (minimum n across animal-state pairs: 36; maximum was n=87). Each session lasts 90 trials. Animals are ordered in the same way as in other supplemental figures so plots can be compared across figures.

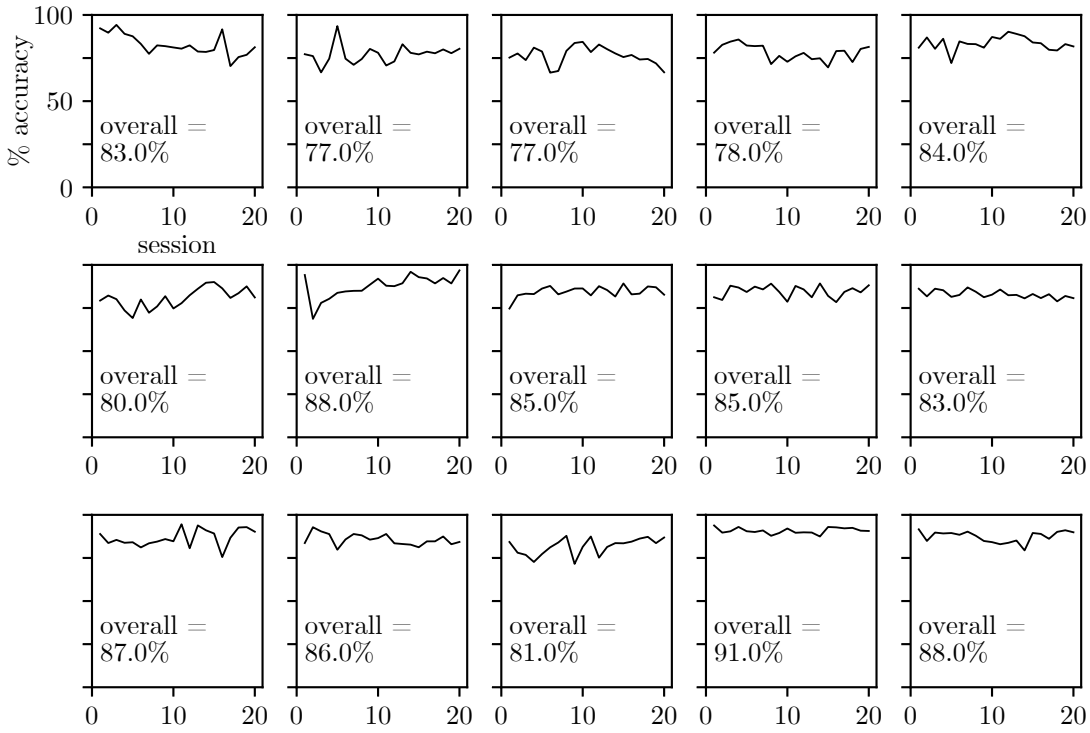

Figure S13: **Accuracy across sessions for Odoemene et al. [4] animals.** We plot the accuracy across sessions for Odoemene et al. animals as evidence that the animals' choice behavior has reached stationarity.

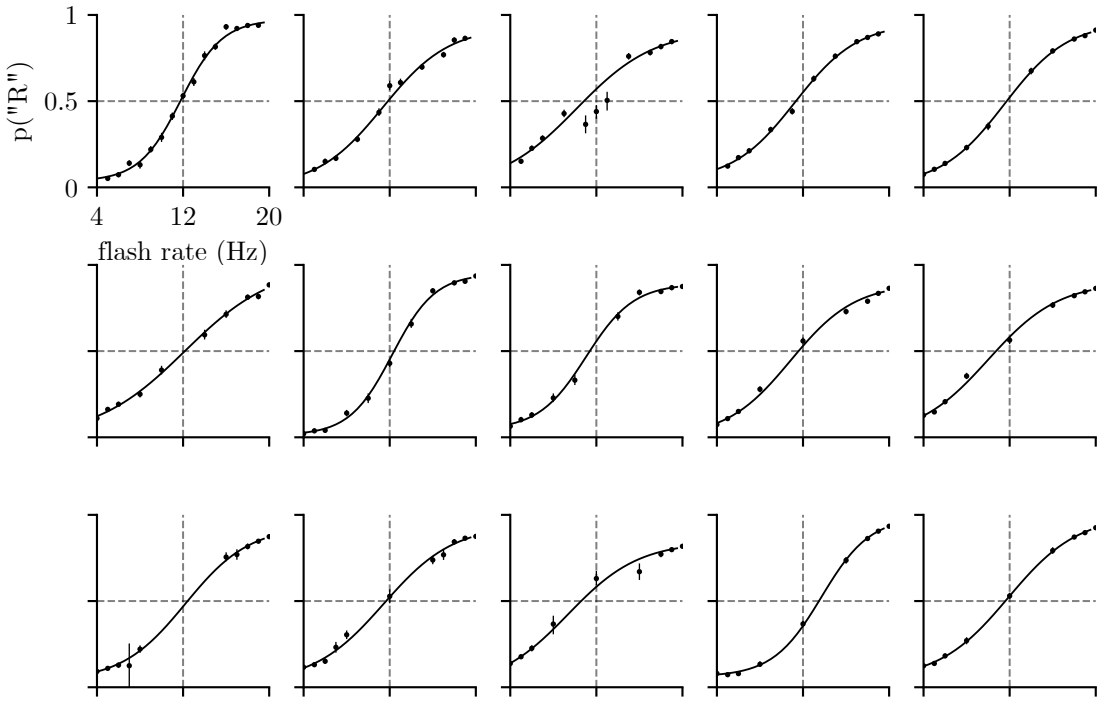

Figure S14: **Psychometric curves for Odoemene et al. [4] animals.** We plot the psychometric curves for each of the 15 animals whose choice data we study. We also show each animal's empirical choice probabilities; error bars are 68% confidence intervals (median n across animal-stimulus pairs was n=1070; minimum was n=8; maximum was n=5253). Animals are ordered as in Fig. S13.

References

[1] The International Brain Laboratory, Valeria Aguillon-Rodriguez, Dora E. Angelaki, Hannah M. Bayer, Niccolò Bonacchi, Matteo Carandini, Fanny Cazettes, Gaelle A. Chapuis, Anne K. Churchland, Yang Dan, Eric E. Dewitt, Mayo Faulkner, Hamish Forrest, Laura M. Haetzel, Michael Hausser, Sonja B. Hofer, Fei Hu, Anup Khanal, Christopher S. Krasniak, Inês Laranjeira, Zachary F. Mainen, Guido T. Meijer, Nathaniel J. Miska, Thomas D. Mrsic-Flogel, Masayoshi Murakami, Jean-Paul Noel, Alejandro Pan-Vazquez, Josh I. Sanders, Karolina Z. Socha, Rebecca Terry, Anne E. Urai, Hernando M. Vergara, Miles J. Wells, Christian J. Wilson, Ilana B. Witten, Lauren E. Wool, and Anthony Zador. A standardized and reproducible method to measure decision-making in mice. *bioRxiv*, page 2020.01.17.909838, January 2020.

[2] Nicholas A. Roy, Ji Hyun Bak, Athena Akrami, Carlos Brody, and Jonathan W. Pillow. Efficient inference for time-varying behavior during learning. In *Advances in Neural Information Processing Systems*, pages 5695–5705, 2018.

[3] Nicholas A. Roy, Ji Hyun Bak, International Brain Laboratory, Athena Akrami, Carlos D. Brody, and Jonathan W. Pillow. Extracting the dynamics of behavior in sensory decision-making experiments. *Neuron*, 109(4):597–610.e6, February 2021.

[4] Onyekachi Odoemene, Sashank Pisupati, Hien Nguyen, and Anne K. Churchland. Visual Evidence Accumulation Guides Decision-Making in Unrestrained Mice. *Journal of Neuroscience*, 38(47):10143–10155, November 2018.